

Text S1. Supplementary Materials and Methods.

Adhesion properties of selected and unselected parasite lines. The rosette frequency (percentage of IE binding two or more uninfected E) of unselected and HBEC-selected parasite lines was determined by microscopy of ethidium-bromide-stained wet preparations as described (1). The clumping frequency (percentage of IE in clumps of three or more IE in the presence of platelets) was determined by microscopy of ethidium-bromide-stained wet preparations (2) with the clumping assay set up at 1% parasitaemia, 10% haematocrit with 20% platelet-rich plasma and incubated for 60 mins at 10 rpm. Spot binding assays were as described (3) with proteins/concentrations as shown in Table S1 (SI Appendix). The IFA for Knobs was carried out on thin smears fixed with 90% acetone/10% methanol and incubated with 10 µg/ml of mAb 89 to KAHRP (4) or IgG2a isotype control for 1h, followed by 3x washes in PBS and secondary incubation for 45 mins with 1/500 dilution of highly cross-absorbed Alexa Fluor 488 goat anti-mouse IgG with 1 µg/ml of DAPI to stain parasite nuclei. After 3x further washed the slides were mounted with Fluoromount and viewed by fluorescence microscopy. 100 IEs were counted for presence/absence of knobs in four separate areas of each slide to give the mean knob positivity and SEM for each strain.

Microarray hybridizations. HBEC-selected parasites were cultured and synchronized alongside their unselected (non-binding) counterpart. At late schizont stage, HB3-HBEC1 and HB3-Uns1 control cultures (pilot experiment) were Percoll-treated to purify IEs (5), while for all other selections, schizont-IEs were purified on a MACS column (6). Five to seven hours later, after most schizonts had ruptured and parasites were mostly at early-ring stage, cultures were sorbitol-treated (7). Time point 1 of a time-course experiment started 8 hours after the end of the Percoll/MACS

treatment (i.e. 1-3 hours after sorbitol treatment). Samples were processed as described previously (8). Briefly, after RNA extraction, a reference pool was created from each unselected strain by pooling an equal amount of RNA from each time point. After reverse-transcription, each time point sample (from selected and unselected populations) was labelled with Cy5 (red) while the reference pool was labelled with Cy3 (green). Samples were then hybridized overnight. The exception to this was a pilot experiment in which each HB3-HBEC1 time point was hybridised directly with HB3-Uns1 time points rather than using a reference pool.

Microarray data were analysed as described (8). Briefly, each array was normalized with Lowess. Only spots with median intensities greater than the local background plus 2 times the standard deviation of the background were used. For data visualisation, the [HBEC-selected/pool] ratios were divided by the [unselected/pool] ratios to obtain [HBEC-selected/unselected] ratios. Data for HB3-HBEC-2 time point 6 is missing due to a technical problem. Data analysis was carried out using Microsoft Excel, MeV (9), Cluster

(<http://bonsai.ims.utokyo.ac.jp/~mdehoon/software/cluster/software.htm#ctv>) and Jalview (<http://jtreeview.sourceforge.net/>) for data visualization. All microarray data have been deposited in the GEO repository (GSE32211):

<http://www.ncbi.nlm.nih.gov/geo/query/acc.cgi?acc=GSE32211>

Real-Time Quantitative (q)PCR. Transcript levels of the *var* genes from 3D7, IT/FCR3 and HB3 parasite strains and the *rif* genes located head-to-head with the group A *var* gene candidate ligands were determined by real-time qPCR performed on a Rotorgene RG-3000 thermal cycler (Corbett Research) as previously described (10, 11). Primers designed to amplify the *rif* genes of the HB3 strain were as follows: PFHG_03235: forward-tgcgaaaagtcgatagcaga, reverse-agccgcttagtagcagcag; PFHG

_03841: forward-catagtgatgccattccaacat, reverse-ccacctattaatccaattctgg; PFHG
_05051/HB3RifA_081:

forward-actgtgggtatgggttaggaagt, reverse-gcttagcaataaccttctctggat; PFHG _03670:
forward-agtgctatgcccgacaattt, reverse-acaccggtttagcatcagc; PFHG _02275: forward-
gatatgttgacataaccttctctgg, reverse-agcgtttgaagaattgcaca. Transcript level differences
between selected and unselected parasite lines were calculated as $\Delta\Delta C_t$ -values and
shown as fold changes ($2^{\Delta\Delta C_t}$) (User Bulletin #2: ABI Prism 7700 Sequence Detection
System; [http://www3.appliedbiosystems.com/cms/groups/mcb_support/documents/
generaldocuments/cms_040980.pdf](http://www3.appliedbiosystems.com/cms/groups/mcb_support/documents/generaldocuments/cms_040980.pdf), Applied Biosystems).

Generation of polyclonal antibodies to HB3var3 NTS-DBL α 1, HB3var3 di-domain and 3D7 PFD0020c NTS-DBL α 1. Recombinant PfEMP1 domains were produced in *E. coli* and purified as described previously (12). The domain boundaries for HB3var3 NTS-DBL α 1 were Met1-Pro468, for HB3var3 di-domain were Met1-Arg762 and for 3D7 PFD0020c NTS-DBL α 1 were Met1-Pro475. Primers were as follows: HB3var3 NTS-DBL α 1 and di-domain forward 5'-aaggatccatggggatcaagcgcatcaaaa-3'; HB3var3 NTS-DBL α 1 reverse 5'-aagctagcttatggacatacttggaataatc-3'; HB3var3 di-domain reverse 5'-aagctagcttagcgcctcattcaattgttg-3'; 3D7 PFD0020c forward 5'-aaggatccatggggacaggttcacaaact-3' and reverse 5'-ttgctagcttagggacagggttggaataatc. Purified proteins with the his-tag removed by TEV protease cleavage (12) were used to immunize rabbits (two per antigen). The rabbits were pre-screened by IFA to exclude animals with heterophilic antibodies that recognise either infected or uninfected Es as described previously (12). All immunizations were carried out by BioGenes GmbH (Berlin, Germany). Rabbits were immunized with 125 μ g of protein

on days 0, 7, 14 and 28. An ELISA 50% end titre of at least 1:25,000 was observed for each anti-serum (BioGenes GmbH).

Generation of polyclonal antibodies to HB3var3 DBL δ 5 and 3D7 PFD0020c DBL γ 6. The HB3var3 DBL δ 5 domain was amplified from HB3 genomic DNA by primers LT510 5'-ggatccctgtgaaatcgtggataaaacactgg-3' and LT511 5'-ctgcccgcctacatggagcacagtattctgcatg-3'. The PFD0020c DBL γ 6 domain was amplified from 3D7 genomic DNA by primers LT23 5'-cggatccc tgtaatggaattaagacacttcttg-3' and LT24 5'-tgcccgcctcgcactttgtgttggtgctg-3'. The products were cloned and expressed in a baculovirus/insect cell system and recombinant protein purified on a nickel affinity column as described (13). Rabbit antiserum was raised by subcutaneous injection of 10-20 μ g protein in complete Freund's adjuvant followed by two boosters of protein in incomplete Freund's adjuvant. Recombinant GammaBindTM G type 2 coupled to SepharoseTM 4B (GE Healthcare) was used to purify IgG according to the manufacturer's instructions.

Flow cytometry with plasma from African children. Isogenic pairs of unselected and HBEC-selected parasites were frozen as trophozoites (14) at 1% parasitaemia. Plasma samples were collected from children attending Kilifi District Hospital between 2006-2010. Ethical approval was granted by the KEMRI Ethical Review Committee (SSC protocol number 1131) and informed consent obtained from the participants parents/guardians. Plasma samples from 10 children admitted with cerebral malaria (*P. falciparum* parasitaemia, fever and Blantyre coma score of ≤ 2 with other causes of coma excluded) were tested along with their age, blood group and date of admission-matched uncomplicated malaria controls (children seen in outpatients or admitted but with no signs of severe malaria). Acute plasma samples were collected at the time of admission to hospital and convalescent samples collected

3-4 weeks later. Flow cytometry was as described (15). Briefly, 11.5µl of ethidium bromide-stained (10µg/ml) parasite culture suspension (2% haematocrit in PBS/0.5% BSA) was incubated with 1µl test plasma in 96-well U-bottomed plates (Falcon, Becton Dickinson, USA) for 30 mins at room temperature (RT). The cells were washed three times with 200µl of PBS/0.5 % BSA by centrifuging at 1000rpm for 3 mins in a Rotanta 460R centrifuge (Hettich Zentrifugen, Germany). 50µl of FITC-conjugated sheep anti-human IgG-Fc (Binding Site, UK) at a 1:50 dilution in PBS/0.5% BSA was added and incubated for 30 mins at RT in the dark. Following three further washes, the cells were re-suspended in 200µl of PBS/0.5% BSA and 1000 trophozoite-IEs acquired from each well on an FC500 flow cytometer (Beckman Coulter, UK). Analysis was done using Flowjo version 7.6.4.

References

1. Deans AM & Rowe JA (2006) *Plasmodium falciparum*: Rosettes do not protect merozoites from invasion-inhibitory antibodies. *Exp Parasitol* 112:269-273.
2. Arman M & Rowe JA (2008) Experimental conditions affect the outcome of *Plasmodium falciparum* platelet-mediated clumping assays. *Malar J* 7:243.
3. Newbold C, *et al.* (1997) Receptor-specific adhesion and clinical disease in *Plasmodium falciparum*. *Am J Trop Med Hyg* 57:389-398.
4. Taylor DW, *et al.* (1987) Localization of *Plasmodium falciparum* histidine-rich protein 1 in the erythrocyte skeleton under knobs. *Mol Biochem Parasitol* 25:165-174.
5. Handunnetti SM, *et al.* (1992) Purification and in vitro selection of rosette-positive (R+) and rosette-negative (R-) phenotypes of knob-positive *Plasmodium falciparum* parasites. *Am J Trop Med Hyg* 46:371-381.
6. Staalsoe T, *et al.* (2003) In vitro selection of *Plasmodium falciparum* 3D7 for expression of variant surface antigens associated with severe malaria in African children. *Parasite Immunol* 25:421-427.
7. Lambros C & Vanderberg JP (1979) Synchronisation of *Plasmodium falciparum* erythrocytic stages in culture. *J Parasitol* 65:418-420.
8. Claessens A, *et al.* (2011) Design of a variant surface antigen-supplemented microarray chip for whole transcriptome analysis of multiple *Plasmodium falciparum* cytoadherent strains, and identification of strain-transcendent *rif* and *stevor* genes. *Malar J* 10:180.
9. Saeed AI, *et al.* (2006) TM4 microarray software suite. *Methods Enzymol* 411:134-193.
10. Wang CW, Magistrado PA, Nielsen MA, Theander TG, & Lavstsen T (2009) Preferential transcription of conserved *rif* genes in two phenotypically distinct *Plasmodium falciparum* parasite lines. *Int J Parasitol* 39:655-664.
11. Soerli J, *et al.* (2009) Human monoclonal IgG selection of *Plasmodium falciparum* for the expression of placental malaria-specific variant surface antigens. *Parasite Immunol* 31:341-346.

12. Ghumra A, *et al.* (2011) Immunisation with recombinant PfEMP1 domains elicits functional rosette-inhibiting and phagocytosis-inducing antibodies to *Plasmodium falciparum*. PLoS ONE 6:e16414.
13. Cham GK, *et al.* (2008) A semi-automated multiplex high-throughput assay for measuring IgG antibodies against *Plasmodium falciparum* erythrocyte membrane protein 1 (PfEMP1) domains in small volumes of plasma. Malar J 7:108.
14. Kinyanjui SM, *et al.* (2004) The use of cryopreserved mature trophozoites in assessing antibody recognition of variant surface antigens of *Plasmodium falciparum*-infected erythrocytes. J Immunol Methods 288:9-18.
15. Bejon P, *et al.* (2009) Analysis of immunity to febrile malaria in children that distinguishes immunity from lack of exposure. Infect Immun 77:1917-1923.

Table S1. Proteins, biomolecules and antibodies used in binding assays.

Protein/molecule/antibody	Supplier/order number	Type	Diluted in	Concentration used
CD36^a	R&D Systems: 1955-CD	Recombinant	PBS	25 µg/ml
Chondroitin sulfate A (CSA)^b	Sigma: C8919	Bovine trachea	PBS	100 µg/ml
E-selectin (CD62E)^c	R&D Systems: 724-ES	Recombinant	PBS	40 µg/ml
Fibronectin^d	BD: 354008	Human plasma	BTC ^q	200 µg/ml
Fibronectin	Sigma: F1141	Bovine plasma	BTC ^q	200 µg/ml
Fractalkine/CX3CL1^e	R&D Systems: 365-FR	Recombinant	PBS	50 µg/ml
gC1qR/HABP1^f	R&D Systems: 4529-HB	Mouse	PBS	40 µg/ml
Heparan Sulfate Proteoglycan^g	Sigma: H4777	Purified	PBS	100 µg/ml
Heparin sodium salt	Sigma: H4784	Porcine intestinal mucosa	50mM Tris	50 µg/ml
Hyaluronic acid^h	Sigma: H1504	Human umbilical cord	2mM CaCl ₂	100 µg/ml
ICAM1 (CD54)ⁱ	R&D Systems: 720-IC	Recombinant	PBS	50 µg/ml
Integrin αV β1	Chemicon : CC1092	Purified	PBS	25 µg/ml
Integrin αV β3^j (CD51)	Chemicon : CC1020	Purified	PBS	25 µg/ml
NCAM (CD56)^k	Chemicon: AG265	Embryonic chicken brain	PBS	10 µg/ml
PECAM-1 (CD31)^l	R&D Systems: ADP6	Recombinant	PBS	50 µg/ml
P-Selectin (CD62P)^m	R&D Systems: 137-PS	Recombinant	PBS	40 µg/ml
Thrombospondinⁿ	Calbiochem: 605225	Purified	50mM Tris	50 µg/ml
VCAM-1 (CD106)^c	R&D Systems: 862-VC	Recombinant	PBS	50 µg/ml
CD36 antibody FA6-152^o	Beckman Coulter IM2279U	Mouse IgG1 mAb	PBS	10 µg/ml
ICAM-1 antibody 15.2^p	AbD Serotec MCA1615XZ	Mouse IgG1 mAb	PBS	20 µg/ml
ICAM-1 antibody 15.8	Gift from Prof Alister Craig	Mouse IgG1 mAb	PBS	20 µg/ml

^a Reference (1, 2)

^b Reference (3)

^c Reference (4)

^d Reference (5)

^e Reference (6)

^f Reference (7)

^g Reference (8)

^h Reference (9)

ⁱ Reference (10). Integrin $\alpha V\beta 1$ was included as a negative control.

^j Reference (11)

^k Reference (12). NCAM was incubated for 2 hours at 37°C with 1U/ml Neuraminidase (Sigma N3001) to digest polysialic acid (PSA) (12).

^l Reference (13)

^m Reference (14)

ⁿ Reference (15)

^o Reference (16)

^p Reference (17)

^q BTC = 50mM Bis-Tris, 100mM NaCl, 25 mM Calcium lactate, 1 mM MnCl₂, pH7.4.

References

1. Oquendo P, Hundt E, Lawler J, & Seed B (1989) CD36 directly mediates cytoadherence of *Plasmodium falciparum* parasitized erythrocytes. Cell 58:95-101.
2. Barnwell JW, *et al.* (1989) A human 88-kD membrane glycoprotein (CD36) functions in vitro as a receptor for a cytoadherence ligand on *Plasmodium falciparum*-infected erythrocytes. J Clin Invest 84:765-772.
3. Fried M & Duffy PE (1996) Adherence of *Plasmodium falciparum* to chondroitin sulphate A in the human placenta. Science 272:1502-1504.
4. Ockenhouse CF, *et al.* (1992) Human vascular endothelial cell adhesion receptors for *Plasmodium falciparum*-infected erythrocytes: roles for endothelial leukocyte adhesion molecule 1 and vascular cell adhesion molecule 1. J Exp Med 176:1183-1189.
5. Eda S & Sherman IW (2004) *Plasmodium falciparum*-infected erythrocytes bind to the RGD motif of fibronectin via the band 3-related adhesin. Exp Parasitol 107:157-162.

6. Hatabu T, Kawazu S, Aikawa M, & Kano S (2003) Binding of *Plasmodium falciparum*-infected erythrocytes to the membrane-bound form of Fractalkine/CX3CL1. Proc Natl Acad Sci U S A 100:15942-15946.
7. Biswas AK, et al. (2007) *Plasmodium falciparum* uses gC1qR/HABP1/p32 as a receptor to bind to vascular endothelium and for platelet-mediated clumping. PLoS Pathog 3:1271-1280.
8. Vogt AM, et al. (2003) Heparan sulfate on endothelial cells mediates the binding of *Plasmodium falciparum*-infected erythrocytes via the DBL1alpha domain of PfEMP1. Blood 101:2405-2411.
9. Beeson JG, et al. (2000) Adhesion of *Plasmodium falciparum*-infected erythrocytes to hyaluronic acid in placental malaria. Nat Med 6:86-90.
10. Berendt AR, Simmons DL, Tansey J, Newbold CI, & Marsh K (1989) Intercellular adhesion molecule-1 is an endothelial cell adhesion receptor for *Plasmodium falciparum*. Nature 341:57-59.
11. Siano JP, Grady KK, Millet P, & Wick TM (1998) Short report: *Plasmodium falciparum*: cytoadherence to alpha(v)beta3 on human microvascular endothelial cells. Am J Trop Med Hyg 59:77-79.
12. Pouvelle B, et al. (2007) Neural cell adhesion molecule, a new cytoadhesion receptor for *Plasmodium falciparum*-infected erythrocytes capable of aggregation. Infect Immun 75:3516-3522.
13. Treutiger CJ, Heddini A, Fernandez V, Muller WA, & Wahlgren M (1997) PECAM-1/CD31, an endothelial receptor for binding *Plasmodium falciparum*-infected erythrocytes. Nat Med 3:1405-1408.
14. Yipp BG, et al. (2007) Differential roles of CD36, ICAM-1, and P-selectin in *Plasmodium falciparum* cytoadherence in vivo. Microcirculation 14:593-602.
15. Roberts DD, et al. (1985) Thrombospondin binds falciparum malaria parasitized erythrocytes and may mediate cytoadherence. Nature 318:64-66.
16. Andrews KT, Adams Y, Viebig NK, Lanzer M, & Schwartz-Albiez R (2005) Adherence of *Plasmodium falciparum* infected erythrocytes to CHO-745 cells and inhibition of binding by protein A in the presence of human serum. Int J Parasitol 35:1127-1134.
17. Berendt AR, et al. (1992) The binding site on ICAM-1 for *Plasmodium falciparum*-infected erythrocytes overlaps, but is distinct from, the LFA-1-binding site. Cell 68:71-81.

Table S2. Summary of selection and synchronisation methods for time-course experiments.

	HB3-HBEC1	HB3-Uns1	HB3-HBEC2	HB3-HBEC TNF ^e	HB3-Uns2	3D7-HBEC	3D7-Uns	IT-HBEC	IT-Uns	Dd2
Rounds of selection ^a	5	/	5	6	/	7	/	6	/	5 ^f
Synchronization method ^b	P + S	P + S	M + S	M + S	M + S	M + S	M + S	M + S	M + S	/
Synchronization window ^c	5 hours	5 hours	7 hours	7 hours	6 hours	7 hours	7 hours	7 hours	5 hours	/
Time between last selection and time-course ^d	13 days	/	12 days	12 days	/	14 days	/	13 days	/	/

^aNumber of rounds of selection on HBEC-5i before the time-course.

^bP = Percoll, S = Sorbitol, M = MACS. See methods section for details.

^cTime between the end of MACS treatment and the Sorbitol treatment. The shorter the time, the more tightly synchronised the parasites are.

^dNumber of days elapsed between the last round of selection and the start of the time-course.

^eHB3 parasites selected on HBEC-5i activated with TNF.

^fThe *P. falciparum* Dd2 strain did not increase its binding ability even after 5 rounds of selection on HBEC-5i.

Table S3. Functional enrichment analysis of down-regulated genes

	Pathway Name	# in Genome	# in Input	# in Pathway	# in Input & Pathway	Direction of deviation from expected	Hypergeometric (to be preferred)	Binomial	Gene List
KEGG pathway testing *	Metabolic pathways	5400	290	259	1	UNDER-representation (expect 13, observe 1)	0.00061	0.00372	PF11110w
GO pathway testing *	GO:0044267 cellular protein metabolic process	5400	290	759	11	UNDER-representation (expect 40, observe 11)	0	0.00001	MAL8P1.70, PFE0370c, PF07_0043, PFD1175w, PFL1885c, PFI0180w, MAL13P1.260, PFL0190w, PFB0665w, PF14_0224, PF14_0027
	GO:0051701 interaction with host	5400	290	8	4	over-representation (expect 0, observe 4)	0.00048	0.00099	PF13_0197, PF10_0345, PF10_0346, PF11_0344
	GO:0030554 adenylyl nucleotide binding	5400	290	368	5	UNDER-representation (expect 19, observe 5)	0.00222	0.00292	PF07_0104, PFD1175w, PFL1885c, PF13_0233, PFB0665w
	GO:0016301 kinase activity	5400	290	292	3	UNDER-representation (expect 15, observe 3)	0.00366	0.00469	PFD1175w, PFL1885c, PFB0665w
	GO:0004175 endopeptidase activity	5400	290	188	3	UNDER-representation (expect 10, observe 3)	0.03094	0.03561	MAL8P1.70, PFE0370c, MAL13P1.260
	GO:0016818 hydrolase activity, acting on acid anhydrides, in phosphorus-containing anhydrides	5400	290	165	1	UNDER-representation (expect 8, observe 1)	0.03181	0.03604	PF10180w
MPM pathway testing*	Functional annotation of merozoite invasion-related proteins	5400	290	60	15	over-representation (expect 3, observe 15)	0	0	PF10_0352, MAL13P1.60, PF10_0351, PF13_0197, PF10_0343, PFL2520w, PFB0570w, PF10_0345, PF10_0281, PFC0110w, PFD1150c, PF10_0346, MAL7P1.176, PF11_0344, PFA0125c
	Subcellular localization of proteins involved in invasion	5400	290	67	12	over-representation (expect 3, observe 12)	0.00019	0.00033	MAL13P1.60, PF10_0351, PF13_0197, PF10_0343, PFL2520w, PF10_0345, PFC0110w, PFD1150c, PF10_0346, MAL7P1.176, PF11_0344, PFA0125c
Testing for Transcription factor*	Transcription Factor								No Transcription Factor(s) are significantly enriched

KEGG: Kyoto Encyclopedia of Genes and Genomes; GO: Gene Ontology; MPM: Malaria Metabolic Pathway. *(level for statistical significance = 0.05)

Table S4. Pair-wise amino acid identities for HBEC-binding variants (whole protein, extracellular domain, NTS-DBL α , CIDR1, DBL δ and CIDR2)

	HB3var3	ITvar7	ITvar19	PFD0020c
Pair-wise amino acid identities for whole protein				
HB3var3	100	36.2	32.5	34.4
ITvar7		100	33.6	45.7
ITvar19			100	41.9
PFD0020c				100
Pair-wise amino acid identities for extracellular domain encoded by exon 1				
HB3var3	100	34.8	29.6	32.8
ITvar7		100	28.5	39.3
ITvar19			100	37.9
PFD0020c				100
Pair-wise amino acid identities for NTS-DBLα				
HB3var3	100	58.1	42.9	49.5
ITvar7		100	45.9	52.1
ITvar19			100	46.5
PFD0020c				100
Pair-wise amino acid identities for CIDR1				
HB3var3	100	74.4	39.2	40.6
ITvar7		100	42.8	40.2
ITvar19			100	74.2
PFD0020c				100
Pair-wise amino acid identities for DBLδ				
HB3var3	100	36.8	37.7	37.9
ITvar7		100	45.4	48.4
ITvar19			100	47.0
PFD0020c				100
Pair-wise amino acid identities for CIDR2				
HB3var3	100	38.9	42.0	24.2
ITvar7		100	47.8	22.3
ITvar19			100	26.5
PFD0020c				100

Table S5. Pair-wise amino acid identities for DBL β and DBL γ from HBEC-binding variants

Pair-wise amino acid identities for DBLβ from HBEC-binding variants						
	HB3var3 d2 ^a	HB3var3 d5 ^b	ITvar7 d2 ^a	ITvar7 d3 ^c	ITvar19	PFD0020c
HB3var3 d2 ^a	100	44.1	52.2	46.4	49.2	49.4
HB3var3 d5 ^b		100	41.4	51.0	46.0	47.1
ITvar7 d2 ^a			100	45.2	50.2	47.2
ITvar7 d3 ^c				100	47.8	46.8
ITvar19					100	58.5
PFD0020c						100
Pair-wise amino acid identities for DBLγ from HBEC-binding variants						
	HB3var3	ITvar7	ITvar19 d3 ^c	ITvar19 d5 ^b	PFD0020c d3 ^c	PFD0020c d4 ^d
HB3var3	100	45.0	49.3	38.7	45.6	47.4
ITvar7		100	33.0	42.7	36.0	56.2
ITvar19 d3 ^c			100	36.3	52.6	38.9
ITvar19 d5 ^b				100	35.7	44.4
PFD0020c d3 ^c					100	39.2
PFD0020c d4 ^d						100

^ad2: 2nd DBL domain from the N-terminus

^bd5: 5th DBL domain from the N-terminus

^cd3: 3rd DBL domain from the N-terminus

^dd4: 4th DBL domain from the N-terminus

Supplementary Figure legends.

Figure S1. Adhesion properties of HBEC-selected parasite lines.

A) The rosette frequency (percentage of IE binding two or more uninfected E) of unselected and HBEC-selected parasite lines was determined by microscopy of ethidium-bromide-stained wet preparations as described (1). The experiment was performed twice for HB3-Uns and HB3-HBEC, once for all other strains. B) The clumping frequency (percentage of IE in clumps of three or more IE in the presence of platelets) was determined by microscopy of ethidium-bromide-stained wet preparations as described (2). The clumping assay was set up at 1% Pt, 10% Ht with 20% platelet-rich plasma and incubated for 60 mins. Data shown are mean and SD from three independent experiments for each strain. There was a significant drop in the clumping frequency after selection for HBEC-binding in all strains (** $p < 0.01$ for each strain, paired t test). C) Spot binding assays with HB3 parasite lines. Three μl spots of soluble receptors in PBS were absorbed overnight onto Falcon 351007 plates. The source and concentration of each molecule is shown in Table S1. Spots were removed by suction and the plates blocked with PBS/2% BSA for two hours. Parasite culture suspension in RPMI binding medium (BM)/1% BSA pH 7.1 at 2% Ht, 5% Pt was incubated with the plates for 1 hour, with gentle resuspension every 12 minutes. Plates were washed gently with BM to remove unbound cells. Bound cells were fixed with 1% glutaraldehyde for 1 hour and stained with 5% Giemsa for 20 mins. The number of adherent IEs were counted in at least five fields of each a spot viewed with the 100x objective. PBS was always used as a negative control, CD36 as a positive control. Data shown are the mean and SD from at

least two independent assays, with each assay comprising at least 3 spots for each molecule per plate, and at least two plates. Statistically significant differences between Uns- and HBEC-selected parasites are shown * $p < 0.05$ ** $p < 0.01$, *** $p < 0.001$. D) Spot binding assays with IT parasite lines as for part C. E) Binding inhibition assay of HB3-HBEC parasites on HBEC-5i in the presence of antibodies known to block adhesion to ICAM-1 (15.2 and 15.8) and CD36 (FA6-152). Data shown are the mean and SD from two independent experiments, with at least two wells per antibody in each experiment.

Figure S2. Parasite maturity during the HB3 time-course. Parasites were synchronized as described in the methods/Table S1 to give a five-hour time window. The first sample was collected 3 hours after sorbitol lysis, and samples were then taken 8-hourly throughout the asexual blood stage cycle. The maximum parasite maturity in terms of hours post invasion at each time point is shown in the second column. Samples for RNA extraction were taken from the culture at each time point, mixed with TRIzol reagent and frozen, and a Giemsa-stained thin blood smear was performed to record the developmental stage of the selected and unselected parasites.

Figure S3. Pearson correlation of time points between selected and unselected parasite strains. Gene transcription data from all oligonucleotide probes from one time point in an unselected strain were correlated with data from all oligonucleotide probes of one time point of the selected strain. A Pearson correlation close to 1 shows a strong positive correlation and a value close to -1 shows a strong negative correlation. Here, in almost all cases, the same time point in an unselected strain showed a strong positive

correlation with the same time point in the selected strain (fields with grey background). The largest disparity was found in time point 3 between HB3-HBEC-TNF and HB3-Uns2 (Pearson correlation coefficient 0.34). Gene expression for that time point should therefore be interpreted cautiously. Time point 6 in the IT strain also showed a relatively weak positive correlation (Pearson correlation coefficient 0.51). All other time points and strains showed a strong positive correlation with correlation coefficients of 0.72 or greater, with many being greater than 0.9.

Figure S4. *Var* gene expression profiles determined by reverse transcriptase-PCR in unselected (Uns) and selected (HBEC) parasites. The pie charts represent the frequency of DBL α *var* gene sequence tags detected in each parasite population by reverse transcriptase-PCR with universal primers to DBL α of PfEMP1 (3, 4). 25 to 45 recombinant plasmids containing *var* gene inserts were sequenced for each strain. A) In HB3-HBEC1 and B) HB3-HBEC-TNF, the frequency of *HB3var3* was increased by 14 and 10 fold respectively in selected compared to unselected HB3 ($p < 0.005$, Fisher's exact test). C) The frequency of *PFD0020c* was increased by 16 fold after selection of 3D7 parasites ($p < 0.0001$, Fisher's exact test). D) In IT-HBEC, *ITvar7* was increased nine fold after selection ($p = 0.0184$, Fisher's exact test) while *ITvar19* was detected in 13/45 sequence tags from IT-HBEC in comparison to 0/38 tags from unselected IT ($p = 0.0001$, Fisher's exact test). E) In HB3 selected four times on HDMEC, the frequency of *HB3var3* increased 11-fold after selection ($p = 0.0015$, Fisher's exact test), while for HB3 selected four times on HPMEC, the frequency of *HB3var3* increased nine-fold ($p = 0.0062$, Fisher's exact test). Colour scheme for *var* subgroups: group A genes are in red,

group B in green, group C in blue. Note that *ITvar19*, a group B *var* gene but with group A-like features, is in orange. Nomenclature: A1T= a *var* gene with the A1 upstream sequence found near the telomeres; C1C= a *var* gene with the C1 upstream sequence found near the centromere. T, telomeric; ST, sub-telomeric; C, centromeric; p, pseudogene.

Figure S5. *Rif* and *stevor* genes upregulated in 3D7- and IT-HBEC selected parasites. A) 3D7 *rif* genes (top of panel) and *stevor* genes (bottom of panel) up-regulated by at least three fold in selected parasites. B) IT *rif* genes (top of panel) and *stevor* genes (bottom of panel) up-regulated by at least three fold in selected parasites. Because of the small size of *rif* genes (1-2 kbp) there was only one oligonucleotide probe per gene on the microarray chip. Colour scale as in main text Fig 2.

Figure S6. 15 genes upregulated in selected parasites in at least one time point by two fold or more in all five selections. Data for each gene represents the average of all available oligonucleotide probes. The top 7 genes are proven or predicted to be exported. “ExportPred” = Export prediction score (5). A score of 4.3 or above corresponds to a 95% chance of the protein to be exported. *PF14_0752* (PHISTa) is the only gene to be upregulated by 3 fold in all selections. t, truncated; p, pseudogene. Colour scale as in main text Fig 2.

Figure S7. 58 genes downregulated in selected parasites in at least one time point by two fold or more in all five selections. Data for each gene represents the average of all available oligonucleotide probes. The gene annotation is according to PlasmoDB 6.4. The annotation “INVASION” or “invasion” was added in order to distinguish proteins proven or predicted to be involved in invasion, respectively (6, 7). The top 11 genes are downregulated by at least 3 fold in one or more time point. Colour scale as in main text Fig 2.

Figure S8. Recognition of HBEC-selected and unselected parasites lines by antibodies from African malaria patients. Convalescent plasma samples were collected from 10 cerebral malaria (CM) patients and 10 age- and time of admission-matched uncomplicated malaria patients (UM or uncomp). Surface recognition of HBEC-selected (HBEC) and unselected (uns) parasite lines was tested by flow cytometry. The mean fluorescence intensity (MFI) of the uninfected E population was subtracted from the MFI of the IE population to give the specific MFI of the IE population shown on the y axis. Each data point represents plasma from one patient. A) 3D7 parasites. B) HB3 parasites. C) IT parasites. D) Summary of median MFI, InterQuartile Range (IQR) and P value from Mann Whitney test for all parasite strains.

References.

1. Deans AM & Rowe JA (2006) *Plasmodium falciparum*: Rosettes do not protect merozoites from invasion-inhibitory antibodies. *Exp Parasitol* 112:269-273.

2. Arman M & Rowe JA (2008) Experimental conditions affect the outcome of *Plasmodium falciparum* platelet-mediated clumping assays. *Malar J* 7:243.
3. Taylor HM, Kyes SA, Harris D, Kriek N, & Newbold CI (2000) A study of *var* gene transcription in vitro using universal *var* gene primers. *Mol Biochem Parasitol* 105:13-23.
4. Kyriacou HM, *et al.* (2006) Differential *var* gene transcription in *Plasmodium falciparum* isolates from patients with cerebral malaria compared to hyperparasitaemia. *Mol Biochem Parasitol* 150:211-218.
5. Sargeant TJ, *et al.* (2006) Lineage-specific expansion of proteins exported to erythrocytes in malaria parasites. *Genome Biol* 7:R12.
6. Hu G, *et al.* (2010) Transcriptional profiling of growth perturbations of the human malaria parasite *Plasmodium falciparum*. *Nat Biotechnol* 28:91-98.
7. Haase S, *et al.* (2008) Characterization of a conserved rhoptry-associated leucine zipper-like protein in the malaria parasite *Plasmodium falciparum*. *Infect Immun* 76:879-887.

A

Unselected parasites	Rosette frequency	HBEC-selected parasites	Rosette frequency
HB3-Uns	<1%	HB3-HBEC	<1%
HB3-Uns2	<1%	HB3-HBEC-TNF	<1%
3D7-Uns	<1%	3D7-HBEC	<1%
IT-Uns	<1%	IT-HBEC	<1%

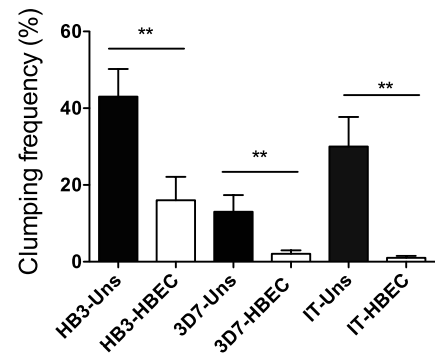
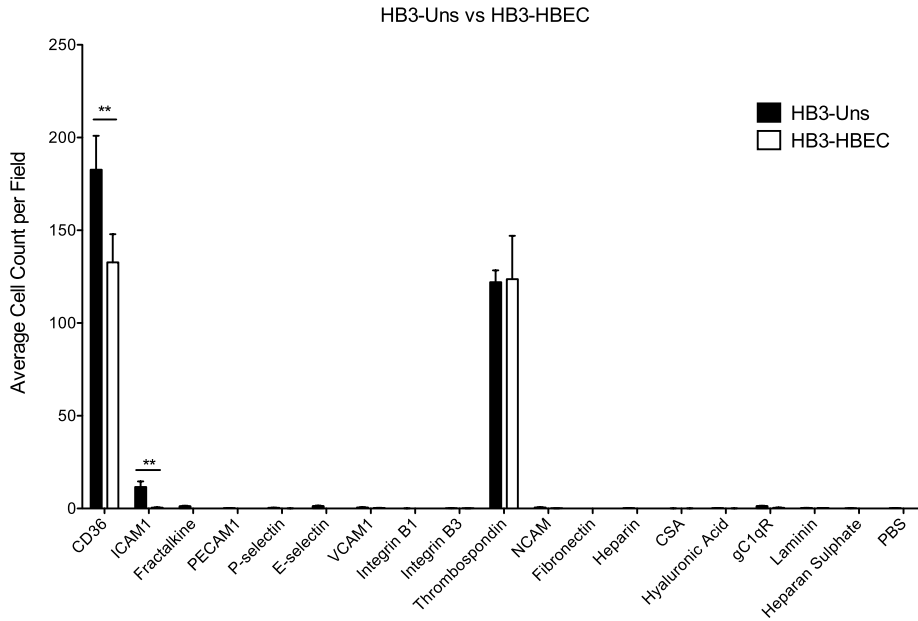
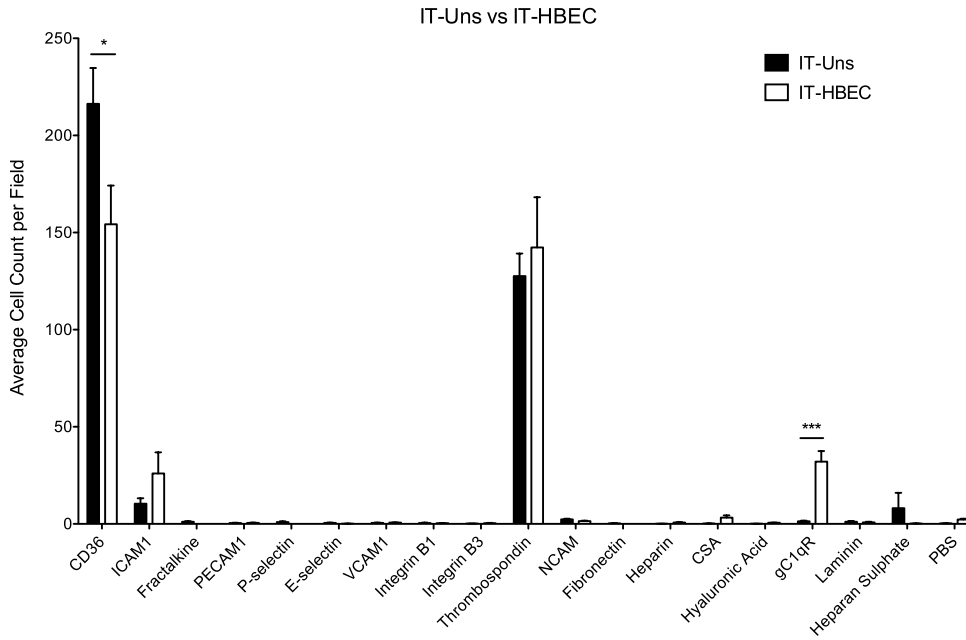
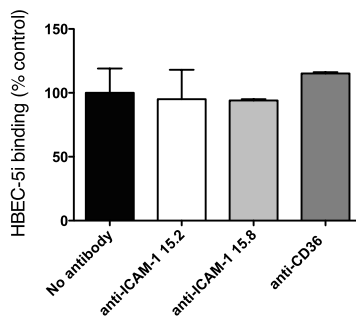
B**C****D****E**

Figure S1

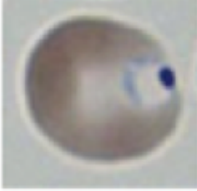


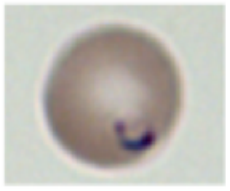


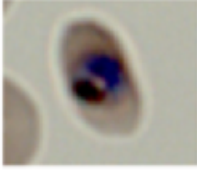
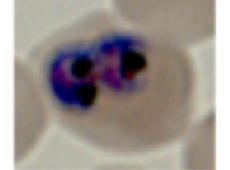

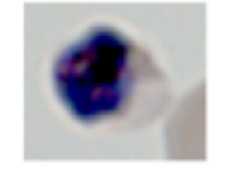
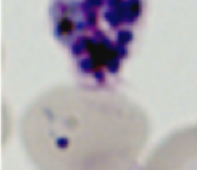

Time-point	Time post invasion	HB3 Unselected	HB3-HBEC Selected
T1 Early ring	8h (range: 3-8h)		
T2 Ring	16h (range: 11-16h)		
T3 Late ring/early troph	24h (range: 19-24h)		
T4 Troph	32h (range: 27-32h)		
T5 Schizont	40h (range: 35-40h)		
T6 Mature schizont	48h (range: 43-48h)		

Figure S2

		HB3-Uns2					
		T1	T2	T3	T4	T5	T6
HB3-HBEC2	T1	0.84	0.66	0.12	-0.20	-0.36	N/A
	T2	0.74	0.86	0.29	-0.18	-0.50	N/A
	T3	0.24	0.65	0.78	0.23	-0.35	N/A
	T4	-0.12	0.11	0.71	0.79	0	N/A
	T5	-0.38	-0.54	-0.10	0.56	0.78	N/A
	T6	N/A	N/A	N/A	N/A	N/A	N/A

		HB3-Uns2					
		T1	T2	T3	T4	T5	T6
HB3-HBEC-TNF	T1	0.88	0.63	0.12	-0.21	-0.32	0.38
	T2	0.26	0.72	0.83	0.28	-0.50	-0.45
	T3	0.73	0.89	0.34	-0.17	-0.51	0.05
	T4	-0.21	0.11	0.71	0.83	-0.09	-0.55
	T5	-0.46	-0.54	-0.07	0.59	0.76	0.1
	T6	-0.01	-0.46	-0.49	-0.11	0.7	0.72

		3D7-Uns					
		T1	T2	T3	T4	T5	T6
3D7-HBEC	T1	0.75	0.77	0.68	0.39	-0.2	-0.3
	T2	0.71	0.88	0.81	0.39	-0.35	-0.48
	T3	0.52	0.73	0.93	0.68	-0.13	-0.51
	T4	0.19	0.38	0.64	0.94	0.40	-0.37
	T5	-0.39	-0.31	-0.17	0.39	0.96	0.33
	T6	-0.24	-0.45	-0.49	-0.26	0.45	0.92

		IT-Uns					
		T1	T2	T3	T4	T5	T6
IT-HBEC	T1	0.91	0.63	0.17	-0.18	-0.37	0.17
	T2	0.84	0.93	0.43	-0.16	-0.58	-0.1
	T3	0.36	0.7	0.92	0.29	-0.46	-0.39
	T4	-0.19	0.03	0.73	0.89	0.18	-0.34
	T5	-0.5	-0.58	-0.12	0.68	0.89	0.11
	T6	-0.33	-0.58	-0.5	0.1	0.86	0.51

Figure S3

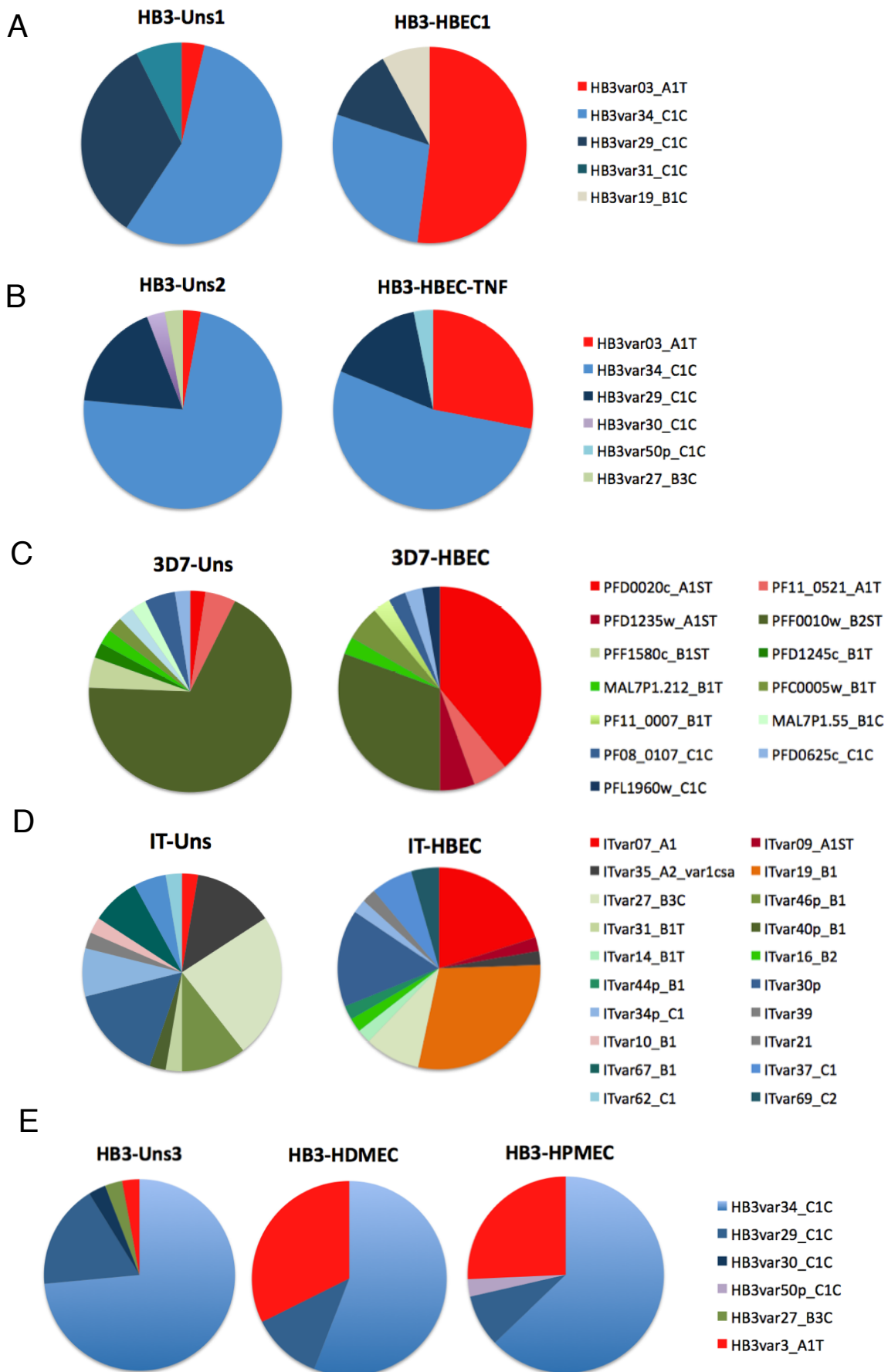
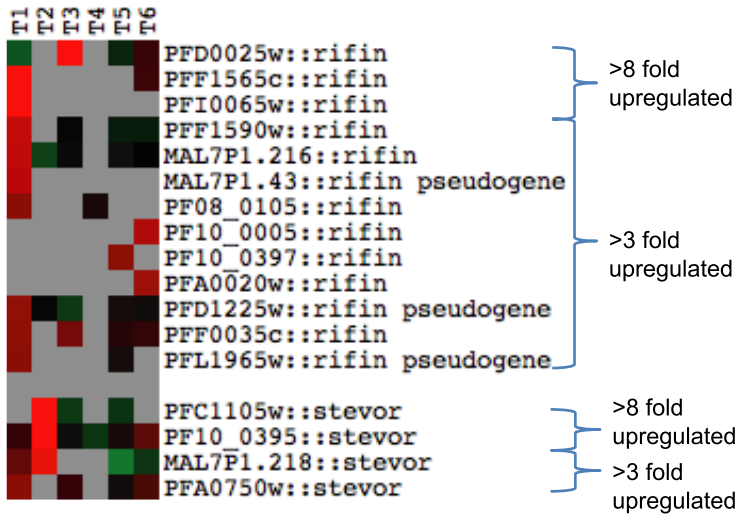
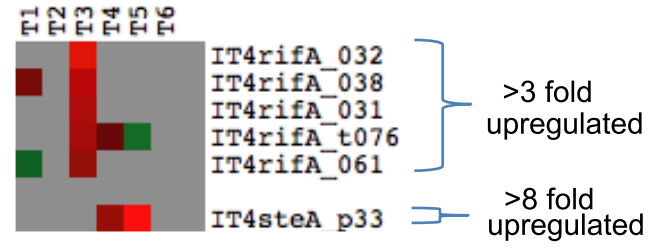


Figure S4

A**B****Figure S5.**

T1	T2	T3	T4	T5	T6	
						HBEC1_PF14_0752:: conserved Plasmodium protein ; ExportPred_12.3; PHISTA
						HBEC2_PF14_0752:: conserved Plasmodium protein ; ExportPred_12.3; PHISTA
						TNF_PF14_0752:: conserved Plasmodium protein ; ExportPred_12.3; PHISTA
						IT_PF14_0752:: conserved Plasmodium protein ; ExportPred_12.3; PHISTA
						3D7_PF14_0752:: conserved Plasmodium protein ; ExportPred_12.3; PHISTA
						HBEC1_PFA0110w::ring-infected erythrocyte surface antigen, RESA; Exported DNAJ type IV PHISTb
						HBEC2_PFA0110w::ring-infected erythrocyte surface antigen, RESA; Exported DNAJ type IV PHISTb
						TNF_PFA0110w::ring-infected erythrocyte surface antigen, RESA; Exported DNAJ type IV PHISTb
						IT_PFA0110w::ring-infected erythrocyte surface antigen, RESA; Exported DNAJ type IV PHISTb
						3D7_PFA0110w::ring-infected erythrocyte surface antigen, RESA; Exported DNAJ type IV PHISTb
						HBEC1_PFB0095c::erythrocyte membrane protein 3, PfEMP3; Exported
						HBEC2_PFB0095c::erythrocyte membrane protein 3, PfEMP3; Exported
						TNF_PFB0095c::erythrocyte membrane protein 3, PfEMP3; Exported
						IT_PFB0095c::erythrocyte membrane protein 3, PfEMP3; Exported
						3D7_PFB0095c::erythrocyte membrane protein 3, PfEMP3; Exported
						HBEC1_MAL13P1.413::membrane associated histidine-rich protein, MAHRP-1; Exported
						HBEC2_MAL13P1.413::membrane associated histidine-rich protein, MAHRP-1; Exported
						TNF_MAL13P1.413::membrane associated histidine-rich protein, MAHRP-1; Exported
						IT_MAL13P1.413::membrane associated histidine-rich protein, MAHRP-1; Exported
						3D7_MAL13P1.413::membrane associated histidine-rich protein, MAHRP-1; Exported
						HBEC1_PF14_0740:: Plasmodium exported protein (hyp17) ; ExportPred_16.5
						HBEC2_PF14_0740:: Plasmodium exported protein (hyp17) ; ExportPred_16.5
						TNF_PF14_0740:: Plasmodium exported protein (hyp17) ; ExportPred_16.5
						IT_PF14_0740:: Plasmodium exported protein (hyp17) ; ExportPred_16.5
						3D7_PF14_0740:: Plasmodium exported protein (hyp17) ; ExportPred_16.5
						HBEC1_PFF0055w:: Plasmodium exported protein (hyp4)
						HBEC2_PFF0055w:: Plasmodium exported protein (hyp4)
						TNF_PFF0055w:: Plasmodium exported protein (hyp4)
						IT_PFF0055w:: Plasmodium exported protein (hyp4)
						3D7_PFF0055w:: Plasmodium exported protein (hyp4)
						HBEC1_PF11_0035::Plasmodium exported protein ; ExportPred_10.1
						HBEC2_PF11_0035::Plasmodium exported protein ; ExportPred_10.1
						TNF_PF11_0035::Plasmodium exported protein ; ExportPred_10.1
						IT_PF11_0035::Plasmodium exported protein ; ExportPred_10.1
						3D7_PF11_0035::Plasmodium exported protein ; ExportPred_10.1
						HBEC1_PF14_0328::mitochondrial import inner membrane translocase subunit tim17, putative
						HBEC2_PF14_0328::mitochondrial import inner membrane translocase subunit tim17, putative
						TNF_PF14_0328::mitochondrial import inner membrane translocase subunit tim17, putative
						IT_PF14_0328::mitochondrial import inner membrane translocase subunit tim17, putative
						3D7_PF14_0328::mitochondrial import inner membrane translocase subunit tim17, putative
						HBEC1_PF14_0651::leucine-rich repeat protein, 14.2
						HBEC2_PF14_0651::leucine-rich repeat protein, 14.2
						TNF_PF14_0651::leucine-rich repeat protein, 14.2
						IT_PF14_0651::leucine-rich repeat protein, 14.2
						3D7_PF14_0651::leucine-rich repeat protein, 14.2
						HBEC1_PFE0400w:: conserved Plasmodium protein, conserved
						HBEC2_PFE0400w:: conserved Plasmodium protein, conserved
						TNF_PFE0400w:: conserved Plasmodium protein, conserved
						IT_PFE0400w:: conserved Plasmodium protein, conserved
						3D7_PFE0400w:: conserved Plasmodium protein, conserved
						HBEC1_PF10_0258:: conserved Plasmodium protein
						HBEC2_PF10_0258:: conserved Plasmodium protein
						TNF_PF10_0258:: conserved Plasmodium protein
						IT_PF10_0258:: conserved Plasmodium protein
						3D7_PF10_0258:: conserved Plasmodium protein
						HBEC1_PF11_0064:: conserved Plasmodium protein
						HBEC2_PF11_0064:: conserved Plasmodium protein
						TNF_PF11_0064:: conserved Plasmodium protein
						IT_PF11_0064:: conserved Plasmodium protein
						3D7_PF11_0064:: conserved Plasmodium protein
						HBEC1_PF14_0383:: conserved Plasmodium protein
						HBEC2_PF14_0383:: conserved Plasmodium protein
						TNF_PF14_0383:: conserved Plasmodium protein
						IT_PF14_0383:: conserved Plasmodium protein
						3D7_PF14_0383:: conserved Plasmodium protein
						HBEC1_PF14_0741:: hypothetical protein
						HBEC2_PF14_0741:: hypothetical protein
						TNF_PF14_0741:: hypothetical protein
						IT_PF14_0741:: hypothetical protein
						3D7_PF14_0741::hypothetical protein
						HBEC1_PFC0345w:: conserved Plasmodium protein
						HBEC2_PFC0345w:: conserved Plasmodium protein
						TNF_PFC0345w:: conserved Plasmodium protein
						IT_PFC0345w:: conserved Plasmodium protein
						3D7_PFC0345w:: conserved Plasmodium protein

Figure S6

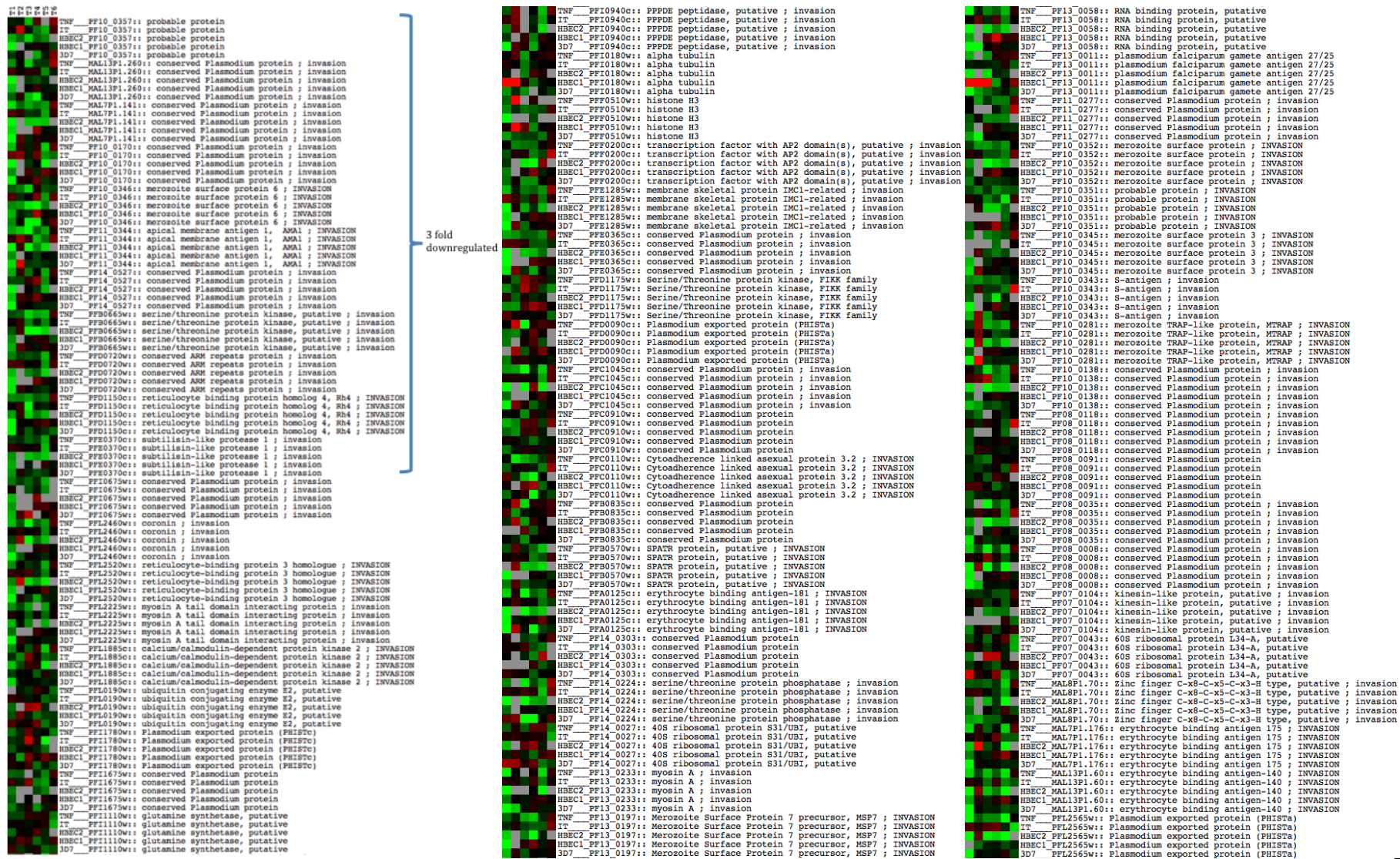
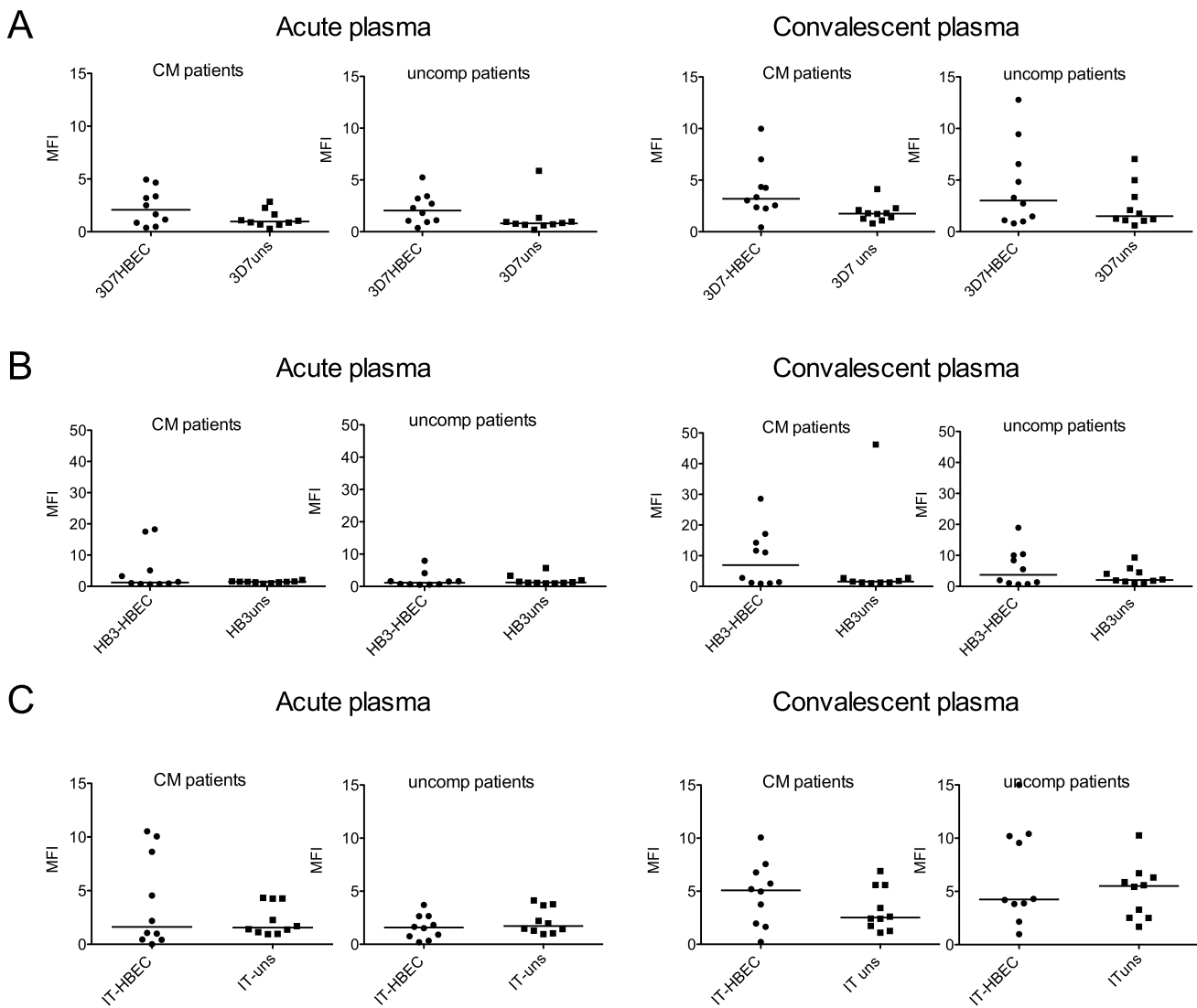


Figure S7



D

	Median MFI HBEC	IQR	Median MFI Uns	IQR	P value
3D7 parasites					
Acute plasma CM	2.08	0.77-3.68	0.97	0.69-1.81	0.17
Acute plasma UM	2.05	1.03-3.27	0.81	0.65-1.06	0.04
Conv plasma CM	3.20	2.30-5.01	1.76	1.22-2.15	0.009
Conv plasma UM	3.02	1.07-7.28	1.50	1.09-3.77	0.44
HB3 parasites					
Acute plasma CM	1.24	0.79-8.22	1.44	1.23-1.57	0.85
Acute plasma UM	1.14	0.64-2.23	1.24	1.06-2.25	0.48
Conv plasma CM	6.92	1.14-14.93	1.57	1.28-2.76	0.60
Conv plasma UM	3.74	0.99-10.12	2.07	4.85	0.74
IT parasites					
Acute plasma CM	1.62	0.44-8.98	1.55	1.09-4.26	1.00
Acute plasma UM	1.58	0.65-2.65	1.72	1.22-3.69	0.35
Conv plasma CM	5.08	1.87-6.96	2.51	1.61-5.58	0.32
Conv plasma UM	4.25	3.41-10.25	5.51	2.52-6.41	0.74

Figure S8